

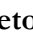







Article

Monitoring Mangroves in Recovery in Porto do Mangue-RN: Effectiveness of RGB and MDE Indices in Drone Images

Leonardo de França Almeida¹, Erivaldo Laurindo Gomes², Renata Ramayane Torquato Oliveira³, Miguel Ferreira Neto⁴, Rogerio Taygra Vasconcelos Fernandes⁵, Raimunda Thyciana Vasconcelos Fernandes⁶, Antônio Gustavo de Luna Souto⁷, Luiz Fernando de Sousa Antunes⁸

¹PhD candidate in Soil and Water Management. Federal Rural University of the Semi-Arid Region . ORCID: 0000-0003-0140-9927. Email: lfaleonardo@hotmail.com

² PhD candidate in Soil and Water Management. Federal Rural University of the Semi-Arid Region . ORCID: 0000-0001-9361-6928. Email: Erivaldo_lgomes@hotmail.com

³ PhD in Soil and Water Management. Federal Rural University of the Semi-Arid Region. ORCID: 0000-0002-7365-8271. E-mail: renataramayanet@gmail.com

⁴ Postdoctoral degree in Plant Physiology. Federal Rural University of the Semi-Arid Region. ORCID: 0000-0002-5128-8230. Email: miguel@ufersa.edu.br

⁵ PhD in Animal Science - Animal Production and Conservation in the Semi-Arid Region. Federal Rural University of the Semi-Arid Region . ORCID: 0000-0002-2901-3986. Email: rogerio.taygra@ufersa.edu.br

⁶ PhD in Animal Science - Animal Production and Conservation in the Semi-Arid Region: Food Technology. Federal Rural University of the Semi-Arid Region. ORCID: 0000-0002-8019-1227. Email: fernandesrtv@hotmail.com

⁷ PhD in Plant Science. Federal Rural University of the Semi-Arid Region . ORCID: 0000-0003-2798-2174. Email: gustavo.luna@ufersa.edu.br

⁸ PhD in Plant Science. Federal Rural University of the Semi-Arid Region. ORCID: 0000-0001-8315-4213. Email: fernando.ufrrj.agro@gmail.com

ABSTRACT

This study evaluated the use of RGB images obtained by Remotely Piloted Aircraft (RPAs) in monitoring mangroves undergoing environmental recovery, located in Porto do Mangue-RN. Six spectral indices (VARI, GLI, MGVRI, MPRI, RGVBI, and ExG) were applied to classify the areas into three thematic classes: exposed soil, ground vegetation, and shrub vegetation. Image processing enabled the generation of orthophotos and Digital Elevation Models (DEM), which provided support for the validation of the results obtained. The spectral indices were tested individually in QGIS software and analyzed in comparison with field data and the DEM. The Excess Green (ExG) index showed greater accuracy and consistency in identifying classes, especially shrub vegetation, reaching values very close to the reference area. The other indices showed limitations, especially in scenarios with high spectral variability and the presence of shadows and wet soil. The use of high-resolution RGB images associated with simple spectral indices proved to be an accessible and efficient tool for monitoring mangrove areas undergoing regeneration, with the potential to support environmental recovery, reforestation, and public preservation policies. The methodology adopted supports environmental management in contexts of limited resources and reinforces the role of ARPs in monitoring sensitive ecosystems.

Keywords: remote sensing; coastal ecosystems; land use and land cover classification; geospatial technology; environmental planning.



Submission: July 21, 2025



Accepted: August 1, 2025



Publication: 09/04/2025



ABSTRACT

This study evaluated the use of RGB images obtained by Remotely Piloted Aircraft (RPA) for monitoring mangroves undergoing environmental recovery, located in Porto do Mangue-RN, Brazil. Six spectral indices (VARI, GLI, MGVRI, MPRI, RGVBI, and ExG) were applied with the aim of classifying the areas into three thematic classes: exposed soil, low vegetation, and shrub vegetation. Image processing allowed the generation of orthophotos and Digital Elevation Models (DEM), which provided support for validating the obtained results. The spectral indices were individually tested using QGIS software and analyzed in comparison with field data and the DEM. The Excess Green Index (ExG) showed the highest accuracy and consistency in identifying the classes, with emphasis on shrub vegetation, achieving values very close to the reference area. The other indices showed limitations, especially in scenarios with high spectral variability and the presence of shadows and wet soil. The use of high-resolution RGB imagery associated with simple spectral indices proved to be an accessible and efficient tool for monitoring mangrove areas under regeneration, with potential to support environmental recovery actions, reforestation, and public preservation policies. The adopted methodology provides support for environmental management in contexts of limited resources and reinforces the role of RPAs in monitoring sensitive ecosystems.

Keywords: remote sensing; coastal ecosystems; land use and land cover classification; geospatial technology; environmental planning

Introduction

Mangroves are coastal ecosystems of great environmental importance, acting as nurseries for various marine and terrestrial species. In addition, they offer protection against erosion and storms (Santos et al. 2021; Souza et al. 2023). These ecosystems also play an essential role in carbon sequestration, storing around 22.8 tons of carbon per year, contributing significantly to climate change mitigation (Santos et al., 2019).

Despite their importance, human activities—deforestation, illegal occupation, pollution, and unsustainable fishing—intensify the degradation of these environments (Duarte and Rezende, 2019). In this context, continuous monitoring of these ecosystems is essential to ensure their conservation and sustainable use, allowing for early detection of changes and the implementation of recovery measures.

Traditional monitoring methods carried out in the field are costly and limited in spatial and temporal coverage (Gomes et al., 2024). Alternatively, satellite images have been used, which offer wide spatial coverage and allow continuous monitoring of large areas over time, with relatively low costs compared to field surveys. However, these images often have limitations, such as low spatial resolution and susceptibility to adverse atmospheric conditions, such as clouds and fog (Santos et al., 2019).

In this scenario, Remotely Piloted Aircraft (RPAs) emerge as a promising technological solution, offering high spatial resolution images, flexibility in data collection, and relatively low cost. This approach has broadened the understanding of the structural dynamics of mangroves (Vikou et al. 2023).

The images obtained by RPAs can operate with different sensors, the most common being RGB sensors, which capture information in the red, green, and blue spectra. Although multispectral and hyperspectral sensors offer a greater wealth of bands, RGB sensors stand out for their accessibility and viability in low-cost monitoring projects. These sensors allow the generation of simple but effective spectral indices, such as Excess Green (ExG) and Vegetation Index from Visible Bands (VARI). Vegetation spectral indices are mathematical formulas applied to image bands (usually red, green, and blue) to highlight the presence and vigor of vegetation in the images. These indices assist in the identification and analysis of vegetation cover and mangrove structure (Phinn et al. 2008; Klemas 2013; Florêncio et al. 2024).

Previous studies, such as those by Costa et al. (2022) and Silva et al. (2024), have demonstrated the potential of using ARPs with RGB sensors to identify degraded areas, successional stages, and regeneration processes in coastal ecosystems. These tools enable the extraction of quantitative information, overcoming some limitations of conventional methods.

Given this context, the objective of this study is to evaluate the potential of using RGB aerial images obtained by ARPs to monitor mangrove areas undergoing recovery. The proposal aims to identify the best

vegetation indices for generating information to support management strategies and environmental recovery actions in mangrove ecosystems .

Materials and Methods

Study area

The study area is located in the rural zone of the municipality of Porto do Mangue, state of Rio Grande do Norte, Brazil, at geographical coordinates $5^{\circ}10'33.83''\text{S}$ and $36^{\circ}45'36.65''\text{W}$ (Figure 1). It is a mangrove forest located within a Permanent Preservation Area (APP), covering an area of approximately 2.85 hectares. The site underwent environmental degradation due to the construction of dikes and the removal of vegetation, and has been undergoing recovery since 2017.

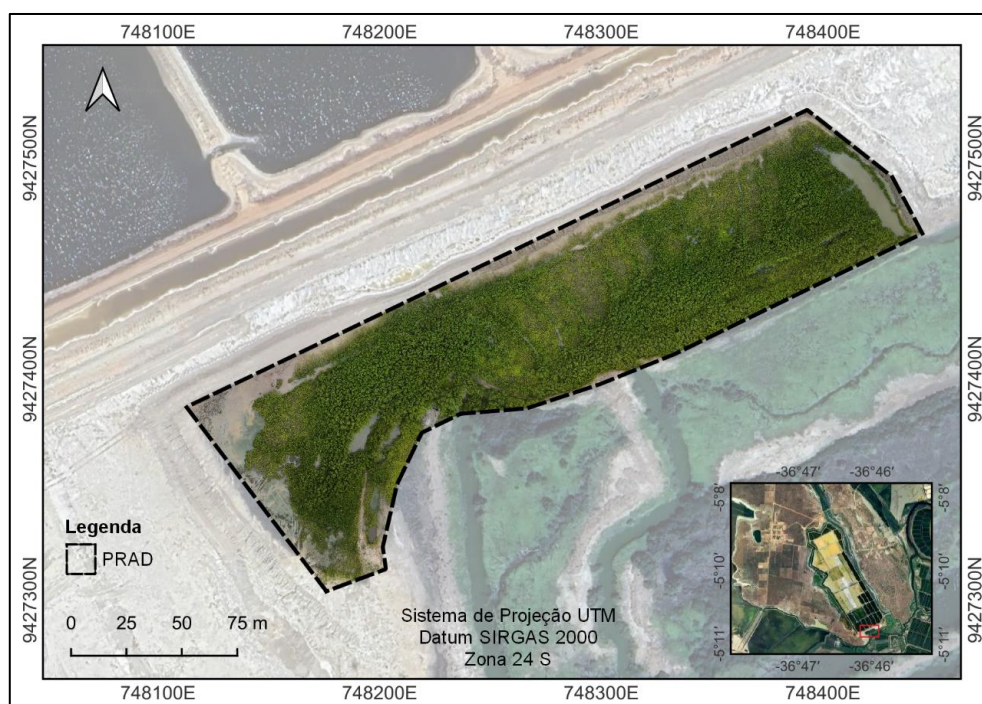


Figure 1 - Map showing the location of the study area. Source: prepared by the authors

Equipment and tools used

A quadcopter-type Remotely Piloted Aircraft (RPA), model DJI Mavic Air 2, was used to collect the information. The images were processed on a mid-range computer equipped with an Intel Core i5 processor, a dedicated graphics card (), and 8 GB of RAM, which proved sufficient to meet the processing demands of the data generated.

Data collection

Data collection was performed based on a field visit and the use of a Remotely Piloted Aircraft (RPA). The purpose of the on-site visit was to directly observe environmental conditions, especially vegetation distribution, in addition to allowing initial data collection (Figure 2).



Figure 2 - Vegetation conditions in the study area, photographic angle a) and photographic angle b). Source: prepared by the authors

During the aerial survey stage, Drone Harmony software was used, which allows for the automation of flight planning and execution (DRONE HARMONY AG 2025) . For this operation, the standard settings of the application were adopted, adjusted according to the perimeter of the area of interest and the flight height. The latter was defined considering the presence of obstacles and the desired spatial resolution, since the flight height directly influences the pixel size of the image obtained. The parameters used in the flight plan are presented in Table 1

Table 1. Information used in the flight plan

Parameters	Lev data (01/21/2025)
Flight altitude	100 m
Flight time	7 min
Number of images	98
Mapped area	3.27 ha
Lateral overlap	70
Front overlap	80
Speed	7 m/s
Spatial resolution	2.00 cm/pixel

Source: prepared by the authors.

The flight consisted of assembling and checking the ARP components, followed by calibration and the start of the automated flyover. The operation was conducted using the aircraft's autopilot system, which followed the previously defined route, altitude, and speed parameters. At the end of the flight, the images obtained were processed to extract the information relevant to the study.

Data processing

DEM and orthophoto generation

After acquiring the images, processing began to generate the DEM and orthophoto. The DEM, which represents the natural relief of the terrain, including ground cover, was fundamental for validating the spectral classification of vegetated areas, serving as a reference factor for determining vegetation size.

The orthophoto, in turn, composed of bands in the RGB spectrum, served as the basis for the application of algebraic operations designed to test classifications using spectral indices. These two products were created using *Agisoft PhotoScan* software, following the steps illustrated in the flowchart below (Figure 3).

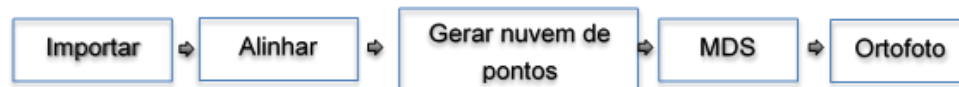


Figure 3 - Steps followed in Agisoft Photoscan to create the DEM and orthophoto using survey images Source: prepared by the authors.

Vegetation indices used for analysis

Once the orthophoto was obtained, it was imported into the QGIS software environment, version 3.40.5, an open-source geoprocessing tool (QGIS 2025). In QGIS, the *Raster Calculator* tool was used to calculate the Vegetation Indices (VIs) listed in Table 2. These indices were derived from mathematical operations between the spectral bands of the orthophoto—red (R), green (G), and blue (B)—generating georeferenced raster layers

that represent different spectral responses of the vegetation. Each index produced was stored as an independent layer, allowing for spatial and comparative analyses.

Table 2. Formulas for Vegetation Indices (VIs) calculated from the RGB spectral bands of the orthoimage

Index Acronym	Index Name (Translation)	Formula	Reference
VARI	Visible Atmospherically Resistant Index	$(G-R)/(G+R-B)$	(Gitelson et al. 2002)
GLI	Global Green Index	$(2G-R-B)/(2G+R+B)$	(Louhaichi et al. 2001)
MGVRI	Modified Green-Red Vegetation Index	$(G)^2-(R)^2/(G)^2+(R)^2$	(Bendig et al. 2015)
MPRI	Modified Photochemical Reflectance Index	$(G-R)/(G+R)$	(Yang et al. 2008)
RGVBI	Red-Green-Blue Vegetation Index	$(R \cdot G)/B^2$	(Bendig et al. 2015)
ExG	Excess Green Index	$2G-R-B$	(Woebbecke et al. 1995)

Source: prepared by the authors.

Image classification

The *r.recode* tool from QGIS, integrated through the GRASS GIS plugin, was used to classify the spectral data. The process began with the creation of a reclassification rules file in txt format, whose content was classified as: "minimum_value:maximum_value:categorical_class," in which specific numerical intervals were defined for three main thematic classes: (1) exposed soil/water, (2) ground vegetation, and (3) shrub vegetation. These rule files were imported into the plugin along with the respective spectral indices.

Each vegetation index was processed individually, generating categorical rasters, in which the original continuous values were converted into integer values representative of the defined classes. This reclassification step enabled the conversion of spectral data into discrete thematic information, which was fundamental for subsequent spatial analyses and for the accurate quantification of the areas occupied by each type of land cover.

The effectiveness of the different indices was evaluated by comparing the results of the automated classification with the field verification data, seeking to identify which index showed greater agreement with the actual conditions observed in situ and with the quantified representation provided by the DEM.

Subsequently, the *r.report* plugin was used to generate descriptive statistics regarding the spatial distribution of the resulting classes. This tool provided quantitative information for each thematic class, expressed in absolute area (hectares) and relative area (percentage of total area), allowing for a detailed analysis of vegetation cover based on each spectral index applied.

Generation of initial products

The photogrammetric processing of the images resulted in the generation of the DEM and the orthophoto in RGB composition. The DEM (Figure 4) revealed altimetric variations ranging from -3.844 m to 1.596 m, allowing the identification of areas most influenced by the tides, corresponding to areas of exposed soil or water, as well as higher regions with shrub vegetation.

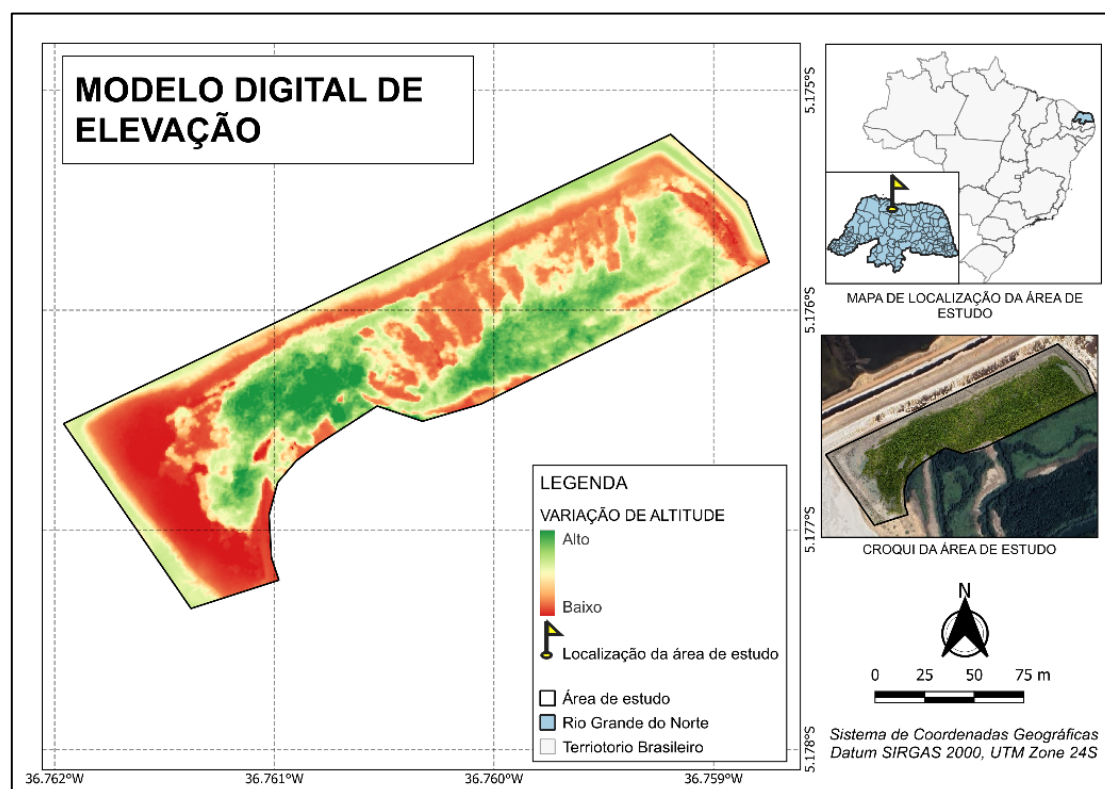


Figure 4 - Digital Elevation Model generated from the field survey with the ARP. Source: prepared by the authors

The RGB orthophoto (Figure 5), with a spatial resolution of 2 cm/pixel, provided sufficient detail for visual distinction of the different land cover classes. The high definition enabled an accurate representation of the distribution and structure of vegetation in the mangrove forest undergoing recovery.

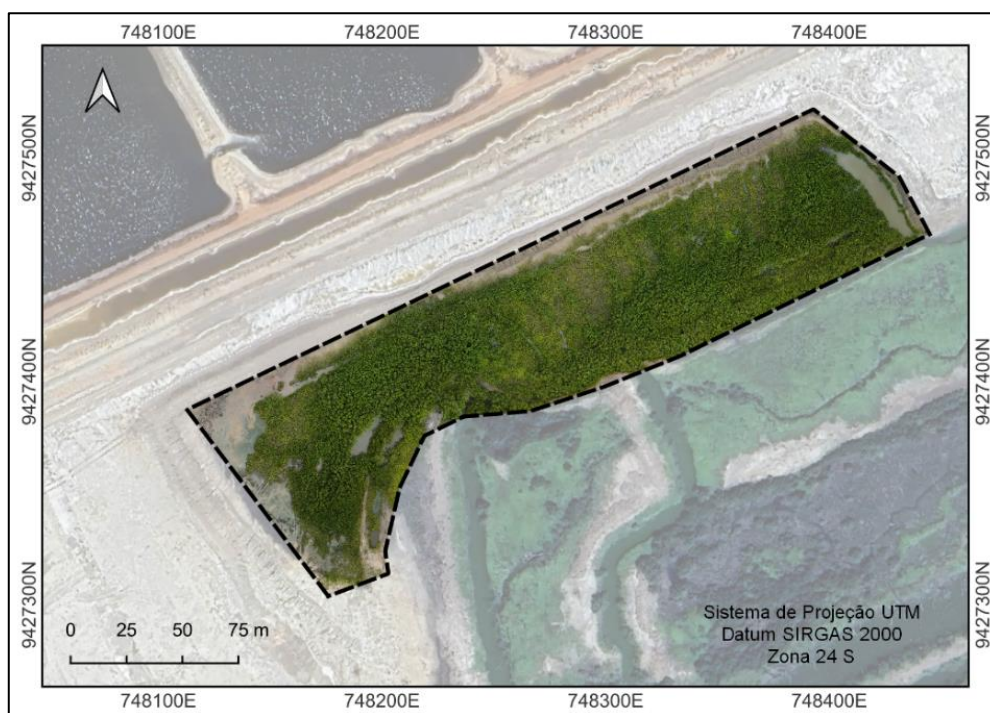
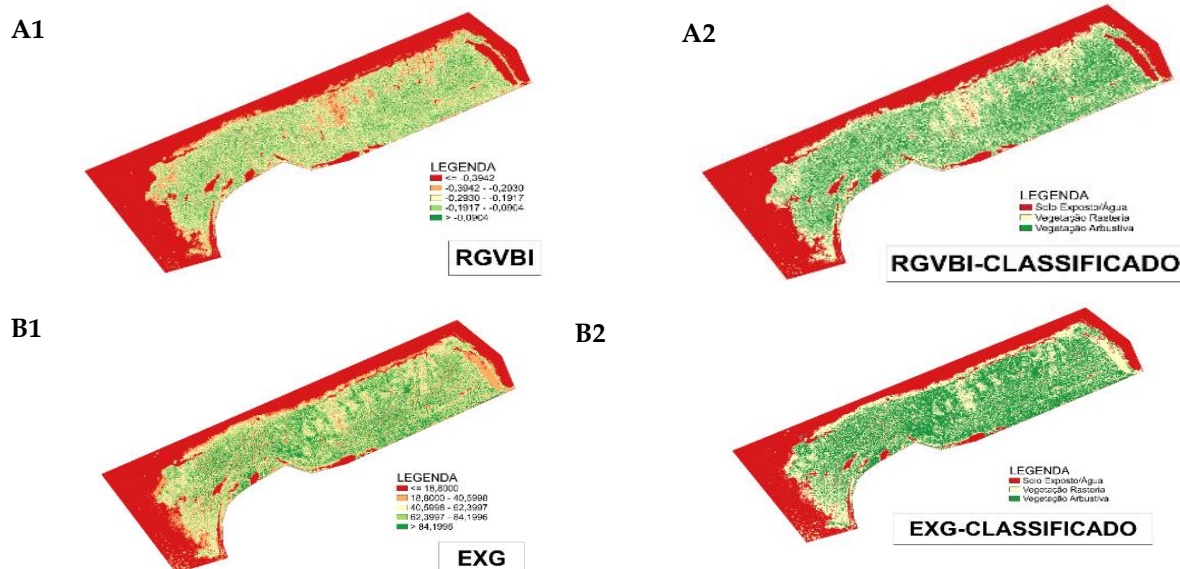


Figure 5 - Orthophoto generated from the processing of data collected by ARP. Source: prepared by the authors

Results and Discussion

Spectral analysis and classification of vegetation cover

Six spectral indices were applied to the RGB orthophoto: RGVBI, ExG, GLI, MGVRI, VARI, and MPRI. Each index resulted in a thematic map (Figure 6), allowing the spectral data to be reclassified into three main categories: exposed soil/water, ground vegetation, and shrub vegetation.



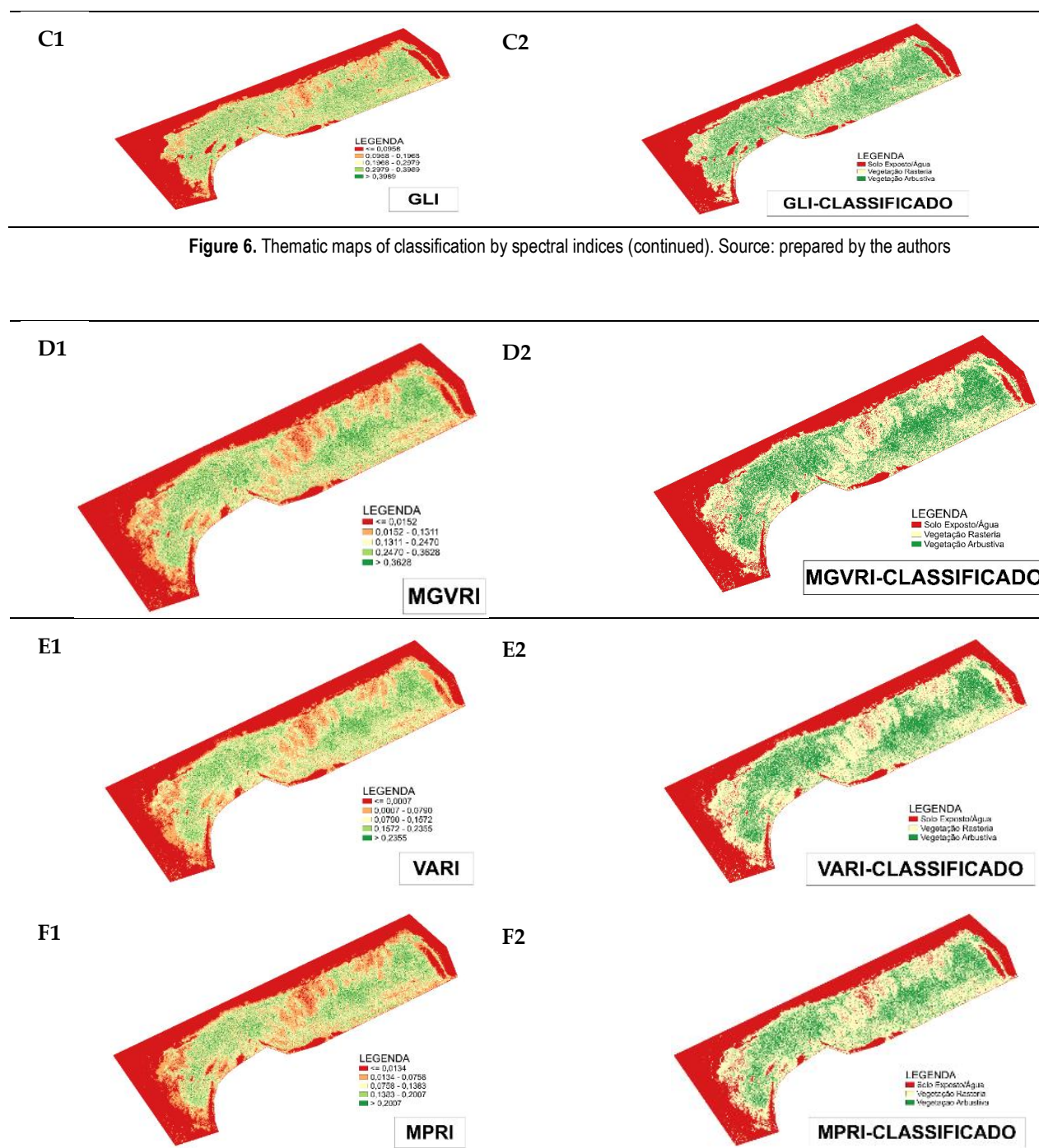


Figure 6. Thematic maps of classification by spectral indices (conclusion). Source: prepared by the authors

The recoding rules used for each index, as well as the respective areas occupied by each class, are presented in Table 3. The distribution of classes varied between indices, reflecting differences in spectral sensitivity .

Table 3. Summary of recoding rules applied to each index and areas accounted for

INDEX	RECODING	AREA ACCOUNTED FOR
RGVBI	-0.6:-0.3942:1	Exposed soil: 1.041486 ha
	-0.3942:-0.1917:2	Undergrowth: 1.060955 ha
	-0.1917:0.6:3	Shrub vegetation: 0.748046 ha
		TOTAL = 2.850486 ha
EXG	-40:18.8000:1	Exposed soil: 0.876912 ha
	18.8000:62.3997:2	Undergrowth: 0.944304 ha
	62.3997:150.0000:3	Shrub vegetation: 1.026303 ha
		TOTAL = 2.847518 ha
GLI	-0.6:0.0958:1	Exposed soil: 1.064864 ha
	0.0958:0.2979:2	Undergrowth: 1.192670 ha
	0.2979:1:3	Shrub vegetation: 0.592982 ha
		TOTAL = 2,850.516 ha
MGVRI	-0.5:0.0152:1	Exposed soil: 1.001772 ha
	0.0152:0.2470:2	Undergrowth: 1.242910 ha
	0.2470:1:3	Shrub vegetation: 0.605816 ha
		TOTAL = 2,850.498 ha
VARI	-0.3:0.0007:1	Exposed soil: 0.954457 ha
	0.0007:0.1572:2	Undergrowth: 1.326321 ha
	0.1572:1:3	Shrub vegetation: 0.569304 ha
		TOTAL = 2.850082 ha
MPRI	-0.6:0.0134:1	Exposed soil: 1.053004 ha
	0.0134:0.1383:2	Ground vegetation: 1.313892 ha
	0.1383:1:3	Shrub vegetation: 0.483619 ha
		TOTAL = 2,850.516 ha

Source: prepared by the authors.

Validation of results and accuracy analysis

Figure 7 shows the map with the delimitation of shrub vegetation based on the DEM, through which it was possible to calculate the extent of vegetated areas with a height greater than 30 cm.

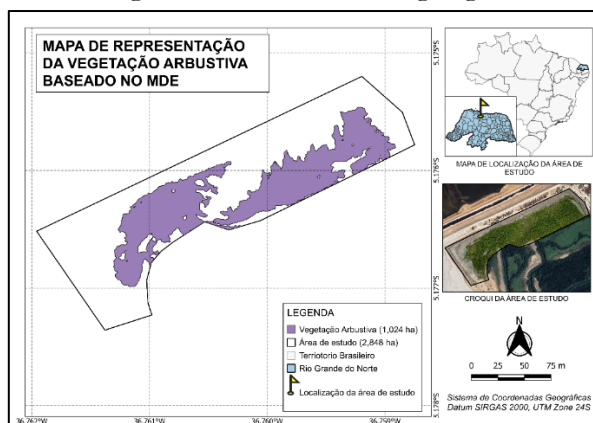


Figure 7 - Map representing shrub vegetation based on the DEM. Source: prepared by the authors

Figure 8 shows the thematic map resulting from the manual selection of vegetated areas, based on the predominant greenish tones in the image. This procedure allowed the visual delimitation of regions with vegetation cover in contrast to areas of exposed soil. The resulting polygons were used to quantify the vegetated area, serving as a validation reference for comparison with the spectral indices derived from the RGB images.

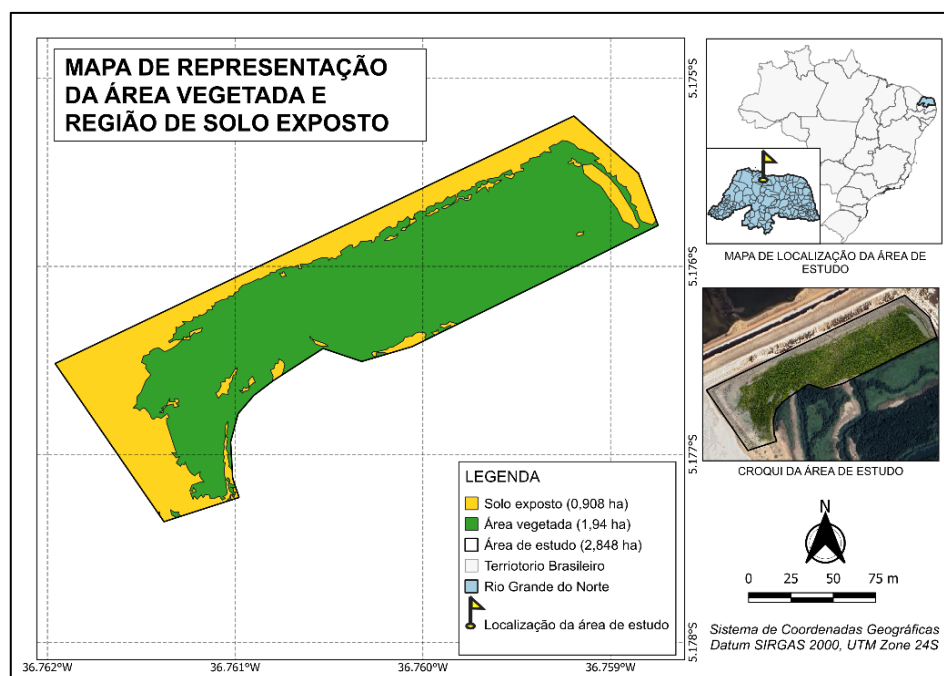


Figure 8 - Map representing the vegetated area and region of exposed soil. Source: prepared by the authors

Table 4 presents a summary of the areas quantified based on the DEM and manual selection of vegetated areas.

Table 4. Summary of quantified reference areas

ID	CATEGORY	AREA
1	Exposed soil	0.908 ha
2	Undergrowth	0.916 ha
3	Shrub vegetation	1.024 ha

Source: prepared by the authors.

The comparative analysis showed that the Excess Green (ExG) index had the highest correspondence with the reference data, demonstrating the best performance in discriminating between the thematic classes evaluated. Among the indices tested, ExG proved to be the most efficient in detecting areas with exposed soil, ground vegetation, and vegetation in advanced stages of regeneration (Figure 8).

Table 5 shows the performance of the spectral indices evaluated for the Exposed Soil, Low Vegetation, and Shrub Vegetation classes, considering the difference between the estimated areas and the reference areas.

The superiority of ExG may be related to its greater sensitivity to the visible green component of the image, which favors the discrimination of areas with shrub vegetation and regeneration in more advanced stages. As shown in the comparative graph and Table 5, ExG was the only index to approach the reference values in the three categories analyzed, with emphasis on shrub vegetation, whose estimate (1.026 ha) was practically identical

to the reference area (1.024 ha). In the exposed soil and ground vegetation classes, ExG also performed consistently, with differences of only -0.031 ha and +0.028 ha, respectively, significantly outperforming the other indices.

The VARI index showed relative accuracy in detecting exposed soil (2nd place, +0.046 ha difference), but failed in ground cover and shrub vegetation, underestimating the latter by -0.455 ha. Studies suggest that VARI is sensitive to interference from shadows and soil moisture, which may explain its inconsistency (Gitelson et al., 2002).

The RGVBI index, on the other hand, performed moderately, overestimating exposed soil (+0.133 ha) and ground vegetation (+0.145 ha), but underestimating shrub vegetation (-0.276 ha). Its formula, based on the ratio between green and blue bands, may be less effective in scenes with high spectral variability (Lussem et al., 2002).

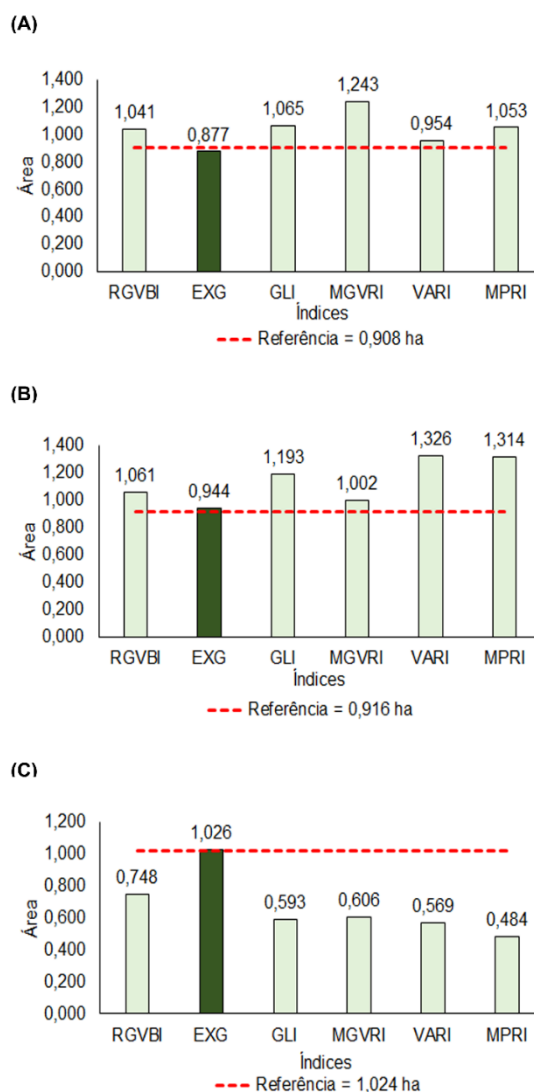


Figure 8- Comparison of the area detected by indices in relation to reference values, A) Exposed soil, B) Ground vegetation, and C) Shrub vegetation.

Table 5. Performance of spectral indices by cover class, considering the difference in relation to the reference area

Class	Position	Index	Estimated value (ha)	Difference in relation to the reference (ha)
<i>Exposed Soil</i>	1	ExG	0.877	-0.031
	2	VARI	0.954	0.046
	3	RGVBI	1.041	0.133
	4	MPRI	1.053	0.145
	5	GLI	1.065	-0.157
	6	MGVRI	1.243	0.335
<i>Undergrowth</i>	1	ExG	0.944	0.028
	2	MGVRI	1.002	0.086
	3	RGVBI	1.061	0.145
	4	GLI	1.193	0.277
	5	MPRI	1.314	0.398
	6	VARI	1.326	0.410
<i>Shrub Vegetation</i>	1	ExG	1.026	0.002
	2nd	RGVBI	0.748	-0.276
	3	MGVRI	0.606	-0.418
	4	GLI	0.593	-0.431
	5	VARI	0.569	-0.455
	6	MPRI	0.484	-0.540

Source: prepared by the authors.

The MPRI and GLI indices were the worst indices for ground cover and shrub vegetation, ranging from 4th to 5th position in each class, indicating limitations in relation to their classification. The MPRI, which mainly uses the red band, is susceptible to spectral noise that can cause overestimation/underestimation in both shrub and ground vegetation, making it difficult to distinguish between these classes. The GLI, based on the green, red, and blue bands, may not adequately capture the structural and spectral variability of dense vegetation, such as shrubbery, and is influenced by exposed soil and environmental variations, which compromises its ability to accurately discriminate between these categories, placing it in the bottom three positions in each class analyzed.

Finally, although the MGVRI index was acceptable for ground vegetation (2nd place, +0.086 ha), it presented a high percentage in exposed soil (+0.335 ha) and shrub vegetation (-0.418 ha), suggesting low robustness in heterogeneous scenarios.

Conclusion

The results of this study demonstrate the potential of using high-resolution RGB images obtained by remotely piloted aircraft (RPAs) to monitor mangrove areas undergoing natural regeneration. The application of six spectral indices (VARI, GLI, MGVRI, MPRI, RGVBI, and ExG) enabled the classification of vegetation cover into three thematic categories—exposed soil, ground vegetation, and shrub vegetation—with variable performance among the indices.

Among the indices analyzed, Excess Green (ExG) stood out for presenting the highest correspondence with the reference data obtained through the Digital Elevation Model (DEM) and the field survey. ExG was

the only index that came closest to the reference values in the three thematic classes, especially in the detection of shrub vegetation, with an estimate practically identical to the validation area. This performance reinforces the sensitivity of ExG to the green component of images, being especially useful in environments with vegetation in intermediate or advanced stages of regeneration. The other indices have specific applications and limitations that must be considered depending on the environmental context and the objectives of the study. The choice of the ideal index should prioritize not only accuracy but also consistency between the classes analyzed.

The approach adopted in this study proved to be an efficient, accessible, and technically feasible alternative for the environmental monitoring of sensitive ecosystems such as mangroves, especially in contexts with limited resources. The information generated can support management strategies, environmental recovery actions, and the formulation of public policies aimed at the preservation of coastal areas.

Qualitative validation based on a combination of Digital Elevation Models (DEM), thematic maps, and field observations provided a robust degree of reliability to the results obtained. To strengthen future analyses, the adoption of georeferenced sampling points and cross-validation with higher resolution spectral data is recommended.

In addition to their scientific value, the results obtained have relevant practical implications. The proposed methodology, based on the use of easily acquired RGB images and simple spectral indices, proved to be an accessible, efficient, and technically feasible alternative for monitoring mangrove areas undergoing regeneration. This information can support reforestation actions, guide environmental management strategies, and support public policies at local and regional scales.

References

- Bendig, Juliane, Kang Yu, Helge Aasen, et al. 2015. "Combining UAV-based plant height from crop surface models, visible, and near infrared vegetation indices for biomass monitoring in barley." *International Journal of Applied Earth Observation and Geoinformation* 39: 79–87. <https://doi.org/10.1016/j.jag.2015.02.012>.
- Costa, Karina Freitas, Etenaldo Felipe Santiago, and Vinicius de Oliveira Ribeiro. 2022. "Use of images in environmental assessment and restoration in natural environments." *Society, Technology, and the Environment: advances, setbacks, and new perspectives* 3. <https://dx.doi.org/10.37885/220408649>.
- DRONE HARMONY AG. 2025. *Automated Drone Inspections Increase Quality & Safety – Reduce Costs*. <https://www.droneharmony.com/>.
- Duarte, Thiago Lima Santana, and Viviane Almeida Rezende. 2019. "Degradation of mangroves in Aracaju/SE (Brazil): socioeconomic impacts on the activity of uçá crab (*Ucides cordatus*) collectors." *Revista Brasileira de Meio Ambiente* 7 (1).
- Florêncio, José Vinicius de Sousa, Maria do Socorro Bezerra de Araújo, Josiclêda Domiciano Galvêncio, and Rodrigo de Miranda Queiroga. 2024. "Estimation of vegetation height with images obtained from drones using artificial intelligence techniques." *Revista Brasileira de Geografia Física* 17 (5): 3736–49.

Gitelson, A. A., Y. J. Kaufman, and D. Rundquist. 2002. "Novel Algorithms for Remote Estimation of Vegetation Fraction." *Remote Sensing of Environment* 80 (1): 76–87.

Gomes, Maria Tereza Uille, Phamella Lorenzen, and Clarissa Bueno Wandscheer. 2024. "Blue carbon: Mangroves, a potential carbon sink for Latin America and the Caribbean." *Revista Estudos Avançados*, no. 40: 149–82. <https://doi.org/10.35588/drc5zx11>.

Klemas, V. 2013. "Remote sensing of emergent and submerged wetlands: an overview." *TAYLOR & FRANCIS* 34 (18): 6286–320. <https://doi.org/dx.doi.org/10.1080/01431161.2013.800656>.

Louhaichi, M, M. M. Borman, and D. E. Johnson. 2001. "Spatially Located Platform and Aerial Photography for Documentation of Grazing Impacts on Wheat." *Geocarto International* 16 (1): 65–70.

Lussem, U, A Bolten, and M. L Gnyp. 2018. "Evaluation of rgb-based vegetation indices from uav imagery to estimate forage yield in grassland". *Symposium "Developments, Technologies and Applications in Remote Sensing"*, advance online publication. <https://doi.org/10.5194/isprs-archives-XLII-3-1215-2018>.

Phinn, Stuart, Chris Roelfsema, Arnold Dekker, Vittoro Brando, and Janet Anstee. 2008. "Mapping seagrass species, cover and biomass in shallow waters: An assessment of satellite multi-spectral and airborne hyper-spectral imaging systems in Moreton Bay (Australia)." *Remote Sensing of Environment* 112: 3413–25. <https://doi.org/10.1016/j.rse.2007.09.017>.

QGIS. 2025. *Quantum GIS - The open source GIS leader*. <https://qgis.org/>.

Santos, Isabela Rodrigues, Norma Ely Santos Beltrão, and Ariadne Reinaldo Trindade. 2019. "BLUE CARBON IN AMAZONIAN MANGROVES: CONSERVATION AND ECONOMIC VALUATION." *Revista Iberoamericana de Economía Ecológica* 31 (1): 18–28. <https://www.raco.cat/index.php/Revibec/article/download/361040/455862/>.

Santos, Nayara Marques, Diógenes Félix da Silva Costa, and Luiz Antonio Cestaro. 2021. "Identification and mapping of provisioning ecosystem services in the Tijupá River mangrove, Maranhão Island (Northeast Region of Brazil)." *Caminhos de Geografia Journal* 22 (29): 276–94. https://www.researchgate.net/profile/Nayara-Santos-7/publication/349699546_identificacao_e_mapeamento_dos_servicos_ecossistemicos_de_provisao_no_manguezal_do_rio_tijupa_ilha_do_maranhao_regiao_nordeste_do_brasil/links/6053c95592851cd8ce4f8bd3/identification-and-mapping-of-ecosystem-services-in-the-mangrove-forest-of-the-tijupa-river-maranhao-island-northeastern-brazil.pdf.

Silva, Cesar, Alan D'Oliveira Correa, and Matheus Kopp Prandini. 2024. *Environmental quality monitoring of restingas in the coast of southern Brazil using high resolution images: a tool for environmental management*. 29. <https://doi.org/10.1590/S1413-415220240002>.

Souza, Alane Santos, Rafael dos Santos Gonçalves, Everton Luís Poelking, Raffael de Almeida, and Sangermano. 2023. "Mapping of mangroves in Todos os Santos Bay." *Proceedings of the XX Brazilian Symposium on Remote Sensing* (Florianópolis-SC), 2359–62. <http://marte2.sid.inpe.br/col/sid.inpe.br/marte2/2023/05.16.13.45/doc/156174.pdf>.

Vikou, Sidney Vincent de Paul, Otacílio Lopes de Souza da Paz, Daiane Maria Pilatti, and Eduardo Vedor de Paula. 2023. "Analysis of Anthropogenic Pressure on Urban Mangroves: Subsidies for Environmental Protection and Land Use Planning." *Society & Nature* 35. <https://doi.org/10.14393/SN-v35-2023-67515>.

Woebbecke, D. M, G. E Meyer, k Von Bargen, and D. A Mortensen. 1995. "Color indices for weed identification under various soil, residue, and lighting conditions." *Transactions of the ASAE*, 259–69.

Yang, Zhengwei, Patrick Willis, and Rick Mueller. 2008. "Impact of band-ratio enhanced awifs image to crop classification accuracy." *National Agricultural Statistics Service Research and Development Division*, 1–20.